Comparison of Thermally Driven Circulations from a Depth-Coordinate Model and an Isopycnal-Layer Model. Part II: The Difference and Structure of the Circulations

YOUNG-GYU PARK

Marine Environment and Climate Change Laboratory, Korea Ocean Research and Development Institute, Ansan, Korea

KIRK BRYAN

Program in Atmospheric and Oceanic Sciences, Princeton University, Princeton, New Jersey

(Manuscript received 6 June 2000, in final form 2 January 2001)

ABSTRACT

Thermally driven ocean circulations in idealized basins are calculated with two well-known model codes, one based on depth-level coordinates and the other based on isopycnal coordinates. In addition, the two models have very different representations of convection. In the level-coordinate model, convective adjustment is used, while in the isopycnal-coordinate model, convection is simulated by a transformation of the surface layer to the layer below. Both models indicate a three-layer structure in the circulation. The lower and middle layers have a flow structure that corresponds with the classical abyssal circulation models. The upper flow is strongly constrained by the buoyancy flux field at the upper surface and the convective parameterization. The model with convective adjustment and level coordinates is dominated by an eastward flow, which sinks to subsurface level at the eastern boundary. It lacks any indication of a surface cyclonic flow, even in the vicinity of sinking at the northern wall. On the other hand, in the model based on density coordinates the eastward surface flow turns to the north at the eastern boundary and forms a pronounced cyclonic circulation at high latitudes. Due to the cyclonic circulation, the coldest surface water is found near the northwestern corner, while in the level model the coldest water is near the northeastern corner. The isopycnal model appears to be a more realistic representation of the real ocean since both wind and the thermohaline circulation are thought to contribute to the North Atlantic subarctic cyclonic gyre.

Although the zonally averaged buoyancy flux produced by the two model codes is the same, the actual patterns of buoyancy flux at the surface are not similar at high latitudes. This suggests that the two types of numerical models would indicate very different air–sea interaction if coupled to atmospheric models and used to simulate climate. The application of the Gent–McWilliams parameterization of mesoscale eddies to the model with z coordinates and convective adjustment reduces the differences between the surface circulation of the two models by a small amount.

1. Introduction

A small number of simple analogs have proven to be extremely valuable in illustrating important processes in the circulation of the World Ocean. One example is the classical abyssal circulation model of Stommel and Arons (1960), later extended by Kawase (1987). Part I of this paper (Park and Bryan 2000) revisits this problem. Using two well-known types of numerical models, the abyssal circulation problem is extended by including the full three-dimensional structure of the thermocline. As in the original theories of the abyssal circulation the effects of wind at the surface are not included. Part I of this paper shows that, contrary to some rather confusing results of earlier numerical studies, the original scaling for a diffusive thermocline proposed by Bryan and Cox (1967) and Welander (1971) predicts poleward heat transport and thermocline depth correctly for a range of the vertical diffusivity over a factor of 200. The discrepancies in the scaling found in earlier studies were traced to the inclusion of wind, which introduces another vertical depth scale (Stommel and Webster 1962; Salmon 1990; and Samelson and Vallis 1997) or violates similarity by the way that the Newtonian restoring condition was applied at the upper surface.

If the overall depth is much greater than the depth of the thermocline, and the Rossby and Ekman numbers are much less than unity, the only important parameter of the abyssal circulation/thermocline model is the vertical mixing. The scaling for a diffusive thermocline implies that solutions for different levels of vertical mixing can be obtained by simply rescaling in the vertical. This property makes this model a good analog for pro-

Corresponding author address: Dr. Young-Gyu Park, Marine Environment and Climate Change Laboratory, Korea Ocean Research and Development Institute, Ansan, P.O. Box 29, Seoul 425-600, Korea.
E-mail: ypark@kordi.re.kr

viding insight into more realistic models and testing numerical codes. The disadvantage of the requirement of numerical calculations is partially offset by the convenience of scaling.

The goal of this paper is to explore aspects of the thermally driven ocean circulation not captured by the zonally averaged properties analyzed in Part I. We have used two types of models: one is based on z coordinates, and the other is based on density coordinates. The first shall be referred to as ''the z model'' and the second as ''the layered model.'' The z model utilizes the Geophysical Fluid Dynamics Laboratory's (GFDL) second Modular Ocean Model (MOM2) code (Pacanowski 1995) and the second uses a layered code developed by Hallberg (Hallberg and Rhines 1996). In many respects the layered model is similar to the more familiar Miami Isopycnal Coordinate Ocean Model code (Bleck and Smith 1990). In this particular application of the layered model we have not used the standard representation of the mixed layer, but a convection parameterization that transforms the surface layer into the layer below.

The geographical domain of the model is bounded by the equator and a line of latitude at 60°N. In the zonal direction it is bounded by two meridians 60 degrees apart. The resolution of the numerical grid is 2°. Two geometries are tested. In one case the model has a uniform depth of 4 km. In the other geometry it has a sloping shelf around all boundaries, except at the equator. The flow is driven by a linear temperature gradient imposed at the upper surface through the Newtonian damping condition (Haney 1974). In the z model horizontal diffusion is suppressed by using the flux-corrected transport method and the two models are configured to be similar. The vertical diffusion is uniform throughout the basin. To resolve the thermocline for the layered model cases in which very low κ is used more layers are adopted. A linearized equation of state depending only on temperature has been used so that buoyancy and temperature are interchangeable. More details are given in Part I. In addition to the experiments described in Part I, cases with the z model utilizing the eddy mixing parameterization by Gent and McWilliams (1990) are also considered.

It was shown in Part I that the two models give similar results for zonally averaged properties of the solutions and obey the same scaling law. In this paper we explore details of the three-dimensional solution. In the DYNAMO Project (DYNAMO Group 1997) several high-resolution models of the North Atlantic were compared. Initial value problems, starting with observed temperature and salinity, were run out for level, layered, and sigma coordinate models. Results agreed in lower latitudes, where the stratification was significant, but departed from each other and observations in subpolar areas where the stratification was weak. Similar results were found for equilibrium solutions for the much simpler case considered here. The layered model and the z model give the same results for well-stratified areas, but the two solutions diverge close to the poleward boundary where convection is important. The analysis shown later in this paper indicates that a very important difference between these two models is the way in which convection is parameterized.

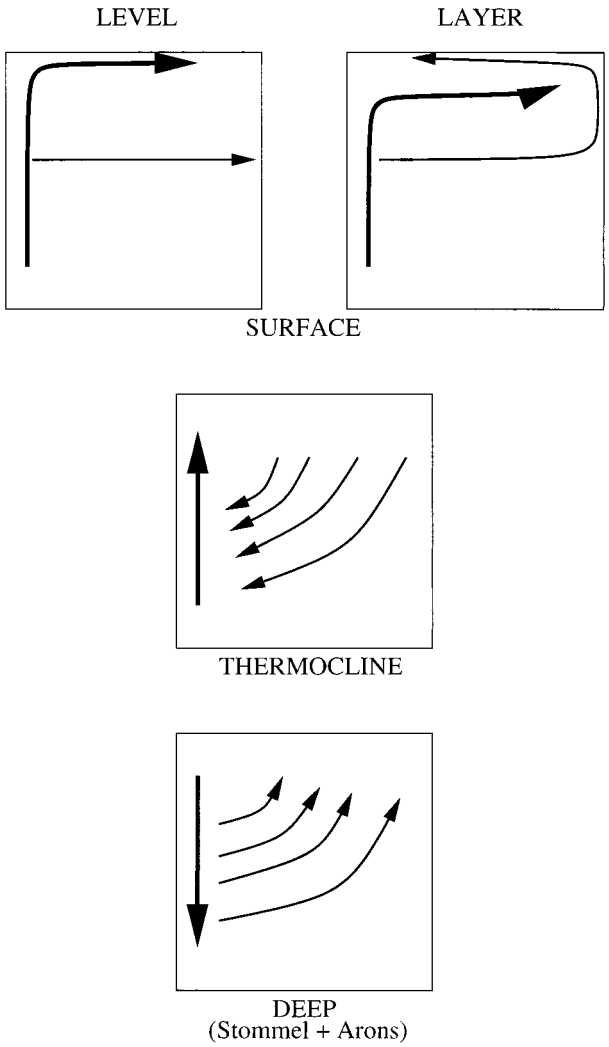

FIG. 1. Schematic diagram of horizontal circulation patterns at different levels.

A schematic of the circulation from the flat bottom cases in Fig. 1 shows the flow pattern at the surface, at an intermediate depth in the middle of the thermocline, and the abyssal flow. Note that the flow pattern at intermediate (or thermocline) and deep levels agrees with a two-layer version of the classical model of Stommel and Arons (1960)/Kawase (1987). At the surface, the direct geostrophic response to the imposition of a zonally uniform, meridional density gradient produces an eastward drift in the interior away from the boundaries. In subpolar latitudes the two models give different circulations. In the case of the z model the eastward drift disappears when it meets the eastern boundary. Sinking is concentrated in the northeast corner of the basin. This

is essentially the same solution that has been shown in previous studies by Cox and Bryan (1984) and Colin de Verdière (1988). As Winton (1996) and more recently Spall and Pickart (2001) point out, this solution is quite unlike the circulation of the North Atlantic. The layered model, however, indicates a less unrealistic surface circulation. The eastward interior flow turns to the north at the eastern boundary. A similar eastern boundary current exists in a laboratory experiment on thermally driven circulations conducted by Park and Whitehead (1999). This eastern boundary current continues cyclonically along the northern wall. The western boundary current separates from the western boundary before it reaches the northern wall, and a cyclonic circulation is generated with sinking located in the northwest corner of the basin. One would expect from simple geophysical fluid dynamics considerations that surface sinking at high latitudes would induce such a cyclonic circulation. Indeed, the thermohaline circulation is thought to play a nearly equal role to that of the wind in driving the observed cyclonic circulation of the North Atlantic subarctic gyre (Luyten et al. 1985).

A key difference between the two models is the existence of a northward flowing, subpolar eastern boundary current in the layered model. A goal of this study is to explore why two popular and well-tested ocean circulation models give different solutions for this standard case. The plan of the paper is first to review the surface circulation in the *z* model and the layered model with an emphasis on the differences in the subpolar area. The difference in the circulation patterns is largely explained by the difference in convective mechanisms in the two models. Next the differences in surface heat flux resulting from the two circulation patterns will be examined, followed by the implications for water mass formation. The three-dimensional structure of the circulation is described in terms of the three levels shown in Fig. 1. Finally we analyze differences in vertical mixing in the *z* model and the layered model.

2. Results

a. Surface circulation

The surface circulation is the key to surface heat balance. Thus details of the surface circulation are very important for the way in which specific features of a model ocean, if coupled to a model atmosphere, will determine air–sea interaction. As shown in Fig. 1, there are significant differences in the surface circulation of the *z* model and layered model in subpolar latitudes. These differences are shown in more detail in Fig. 2. Figures 2a and 2d are the standard, uniform depth cases for the *z* model and layered model, respectively. Figures 2b and 2e are the corresponding cases with shelves along the boundaries except the equator. For the *z* model an additional case is shown in Fig. 2c in which the Gent and McWilliams (1990) eddy mixing parameterization is included in the standard uniform depth case.

In lower latitudes the surface circulation is very much alike for all five cases. There is a western boundary current and a nearly uniform eastward drift in the interior. Surface outcropping in the layered model causes the eastward drift to be less uniform with latitude than in the *z* model. This effect can be lessened by adding more layers, which makes the density jump across an outcrop smaller. In the subpolar region there is a small region of cyclonic circulation in Figs. 2b, 2d, and 2e, but it is missing in the flat bottom cases for the *z* model (Figs. 2a,c). This is the important difference shown in the schematic diagram in Fig. 1. In the flat bottom case for the *z* model the western boundary current extends poleward right to the polar boundary and continues eastward along the polar boundary. In the layered model there is an intensified poleward current along the eastern boundary at high latitudes that continues westward along the polar boundary. This characteristic of the GFDL-MOM code has been noted by Winton (1997) and Spall and Pickart (2001), who both demonstrated that the addition of a shelf permitted a cyclonic circulation as shown in Fig. 2b. The addition of the GM parameterization in the *z* model causes thickness mixing. This relaxes the artificially abrupt fronts created by convective mixing in the *z* model to some extent, but fails to create a cyclonic surface gyre at the northern wall. The eastward drift adjacent to the polar boundary is reduced to some degree compared to Fig. 2a, and the flow near the eastern boundary at high latitudes has a slight poleward component. Increasing the level of thickness mixing in the GM parameterization is not a viable option because it produces excess smoothing of the circulation patterns.

A key difference between the surface circulation of the *z* model and the layered model is the surface flow in the vicinity of the eastern boundary at high latitudes. This is shown in more detail in Fig. 3 for vertical sections adjacent to the eastern boundary. For the *z* model there is a gradual loss of stratification to the north. In subpolar latitudes the stratification vanishes completely above 600 m. The velocity profiles are shown by heavy dark lines, which indicate that the poleward surface flow weakens as the vertical stratification weakens with increasing latitude. This type of circulation has already been described in previous papers by Cox and Bryan (1984) and Colin de Verdière (1988). In contrast the layered model solution shown in Fig. 3b has poleward motion at the surface, which actually intensifies with increasing latitude. The vertical shear of the current is much greater at all latitudes. Note that the vertical stratification in the layered model also weakens, but is still present all the way to the polar wall of the basin.

How different convection parameterizations transform a stratified water column along the eastern wall in the two models is illustrated schematically in Fig. 4. Fig. 4a represents the *z* model and Fig. 4b represents

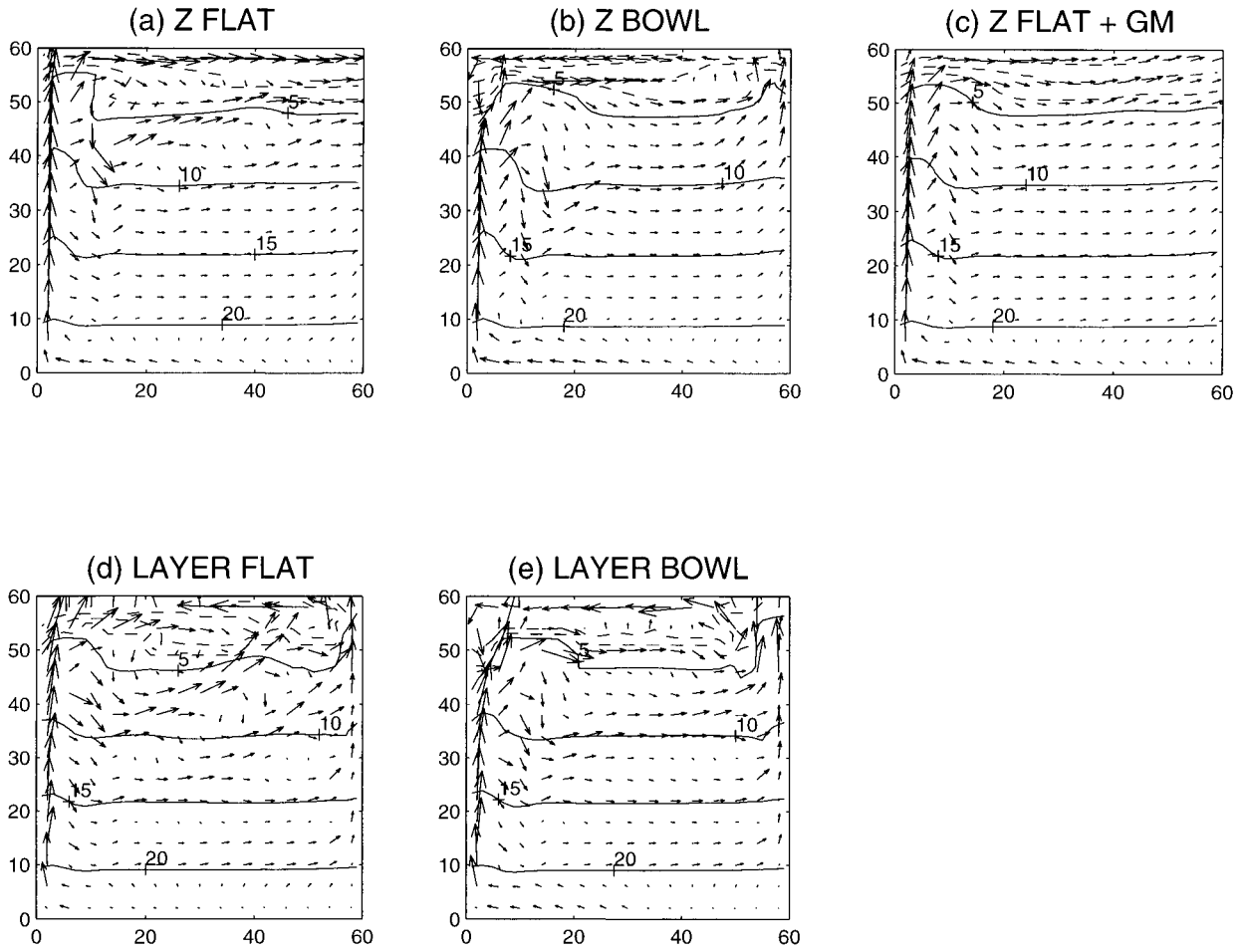

FIG. 2. Surface circulation and surface temperature distribution (the first level for the z model, and the average of the upper 25 m in the layered model) when $\kappa = 1 \times 10^{-4}$ m s^{-2} from (a) the z-model flat-bottom case, (b) the z-model bowl-shaped basin case, (c) the z-model flat-bottom case with the Gent and McWilliams (1990) mesoscale eddy mixing parameterization, (d) the layered-model flat-bottom case, and (e) the layered-model bowl-shaped basin case. An arrow of 1° long is 0.01 m s^{-1}.

the layered model. Assume a column of stratified water in the south. Initially the layers and the levels are assumed to be the same thickness and have the same temperature as shown on the left-hand side of the figure. Let us take 0°C as a reference state and one $\rho_o C_P$ to be an arbitrary unit of heat per unit area within the layers or levels, where ρ_o is reference density of seawater and C_p is the specific heat content of the water. For example, the initial heat anomaly of the top level to the left in a unit area in both the z model and layered model is 25 m^3 × 20°C, or 500 units of heat. The lower layers are at lower temperatures, and so have proportionately lower heat content. In Fig. 3, the stratified surface water in the south (e.g., near 15°N) moves to the north along the eastern wall. Therefore we can assume that the stratified water in this simple example is translated to the north where the air is cold, and 50 units of heat is taken from the surface. As shown in Fig. 4, the finite difference coordinate systems of the layered model and z model respond in quite different ways to this surface heat loss due to the different convective parameterizations in the models. In the case of the z model the heat loss of 50 units makes the upper layer 18°C, which is cooler than the second level. Convective adjustment becomes active and homogenizes the two levels to form homogeneous water of 18.5°C.

In the layered model convection is handled in quite a different way. Heat exchange at the surface induces mass exchange between layers. Cooling at the surface causes the upper layer to grow thinner and the next layer below to increase in volume. Due to the heat loss the upper layer vanishes altogether and the next layer becomes the surface layer, yielding 25 units heat as shown in the diagram. This 25 units is not large enough to account for the imposed heat loss, so the new surface layer starts to thin while the layer below thickens, yielding another 25 units. More detail on surface boundary condition and change in layer thickness can be found in Hallberg (2000). Compared to the z model case, the layered model maintains some stratification near the sur-

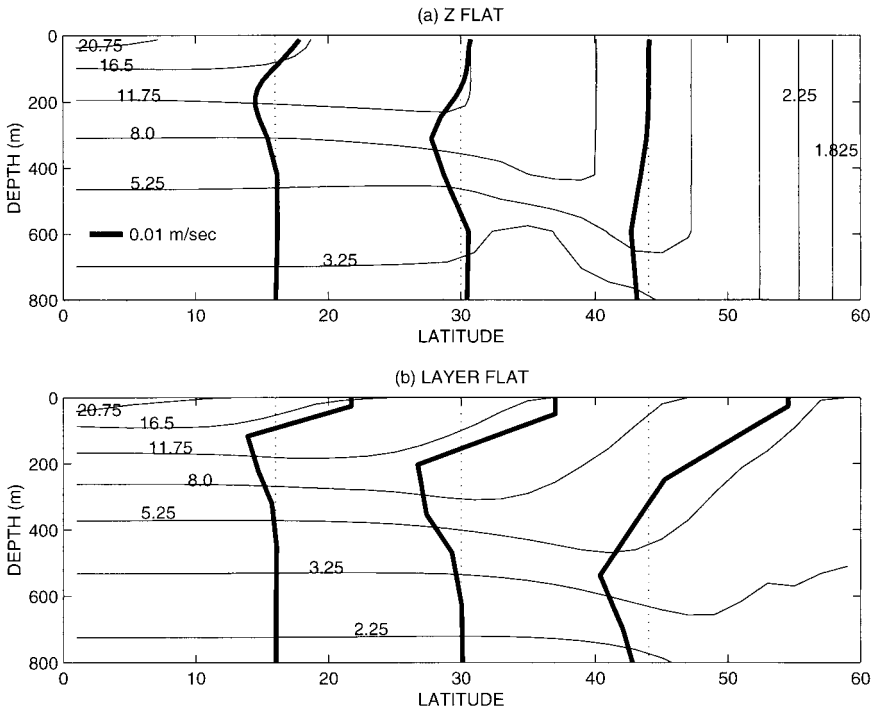

FIG. 3. Meridional T section (contour lines) and V (profiles) along easternmost grid points from (a) the *z* model, and (b) the layered model when $\kappa = 1 \times 10^{-4}$ m s^{-2}. Contour lines are derived from the interface densities of the layered model. Note that contour intervals are not even.

face and allows more baroclinic structure, as in Fig. 3. As we move farther to the north, the convectively mixed layers, of course, become cooler and deeper in both models.

In the simplified, illustrative example in Fig. 4 the advection is greatly simplified, but it offers some insight as to why the patterns of velocity and temperature shown in Fig. 3 for the eastern boundary are so different for the same Newtonian forcing in both cases. When the eastward zonal flow meets the eastern wall, the lack of stratification allows the water to downwell freely and the condition of no normal flow at the wall is satisfied. In the case of the layered model downward motion is resisted by the stratification. As sketched in Fig. 1, the zonal flow from the west becomes a poleward flowing boundary current, analogous to the Norwegian Current in the North Atlantic. As pointed out by Luyten et al. (1985), from observations less than half of the transport of the poleward branch of the North Atlantic subpolar gyre can be accounted for by wind-driven transport; the remainder appears to be associated with the thermohaline circulation. Winton (1997) has pointed out this behavior of the *z* model and has shown that it can be corrected by adding a shelf at the eastern boundary, as shown in Fig. 2b. In the shelf case our calculations show such a poleward flow, but the flow is unstratified. It appears that the topography of a shallow shelf in the *z* model is playing an analogous role to stratification in the layered model.

It is important to consider alternative explanations for the difference in the surface circulation of the layered model and *z* model. The *z* model is based on the Arakawa B grid, while the layered model is based on the Arakawa C grid. When a grid size is larger than the radius of deformation as in this experiment, the B grid gives a more accurate representation of geostrophic adjustment than the C grid (Bryan 1989). Although this may be a factor in the difference in the circulation patterns in the two models, it is probably not the decisive factor, since Fig. 3 shows that both models support poleward boundary currents in low latitudes where the ocean is well stratified and convection is not a major factor.

An important result of Part I is that the zonally integrated properties of the model are in remarkable agreement in spite of differences in the circulation of the *z* model and the layered model. The zonal compensation that permits this behavior is illustrated in Fig. 5, which shows the surface poleward velocity at 30°N. The most intense western boundary current is found in the *z*-model solution (the dashed curve), while a poleward eastern boundary current is absent. On the other hand, the layered model (the solid line) has a less intense western boundary current and a less intense countercurrent and a significant eastern boundary current. Also shown in Fig. 5 is the meridional flow in the case of the *z* model with the GM parameterization added (the dotted line). For a GM thickness mixing coefficient of 10^3 m^2 s^{-1} the poleward velocity profile is not changed signifi-

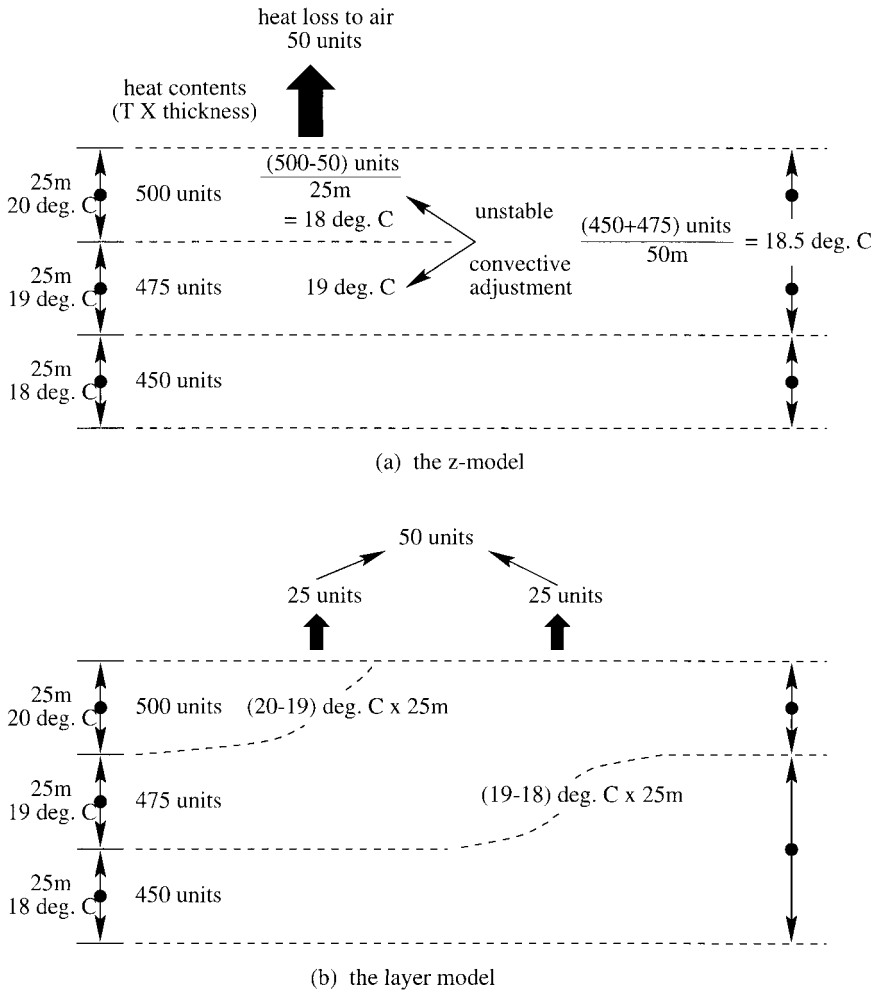

FIG. 4. Diagram of evolution of stratification under heat loss in (a) the *z* model and (b) the layered model.

cantly, but there is a slight tendency to weaken the western boundary current and a slight tendency toward a higher poleward velocity at the eastern boundary. This tendency is increased when a horizontal mixing coefficient of 10^4 m^2 s^{-1} is used. The GM parameterization tends to offset the differences between the solutions caused by the two types of vertical coordinate systems and the two types of convective parameterizations. Essentially the GM parameterization mixes stratification along density surfaces and releases available potential energy stored in the stratification. This tends to offset the sharp boundaries between stratified and unstratified areas created by convective adjustment, allowing weak stratification to appear at the eastern boundary, which

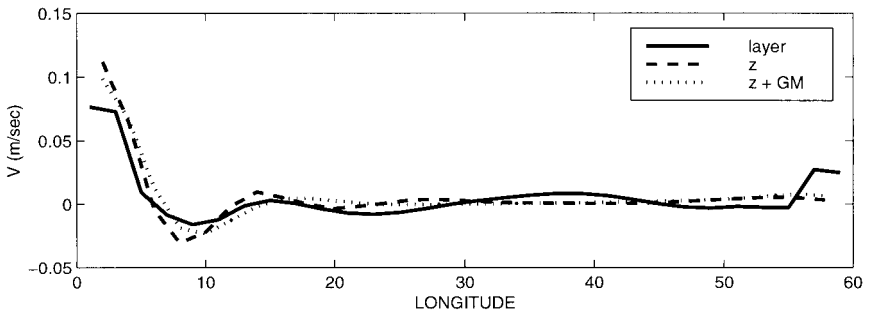

FIG. 5. Meridional velocity (v) at the surface along 30°N.

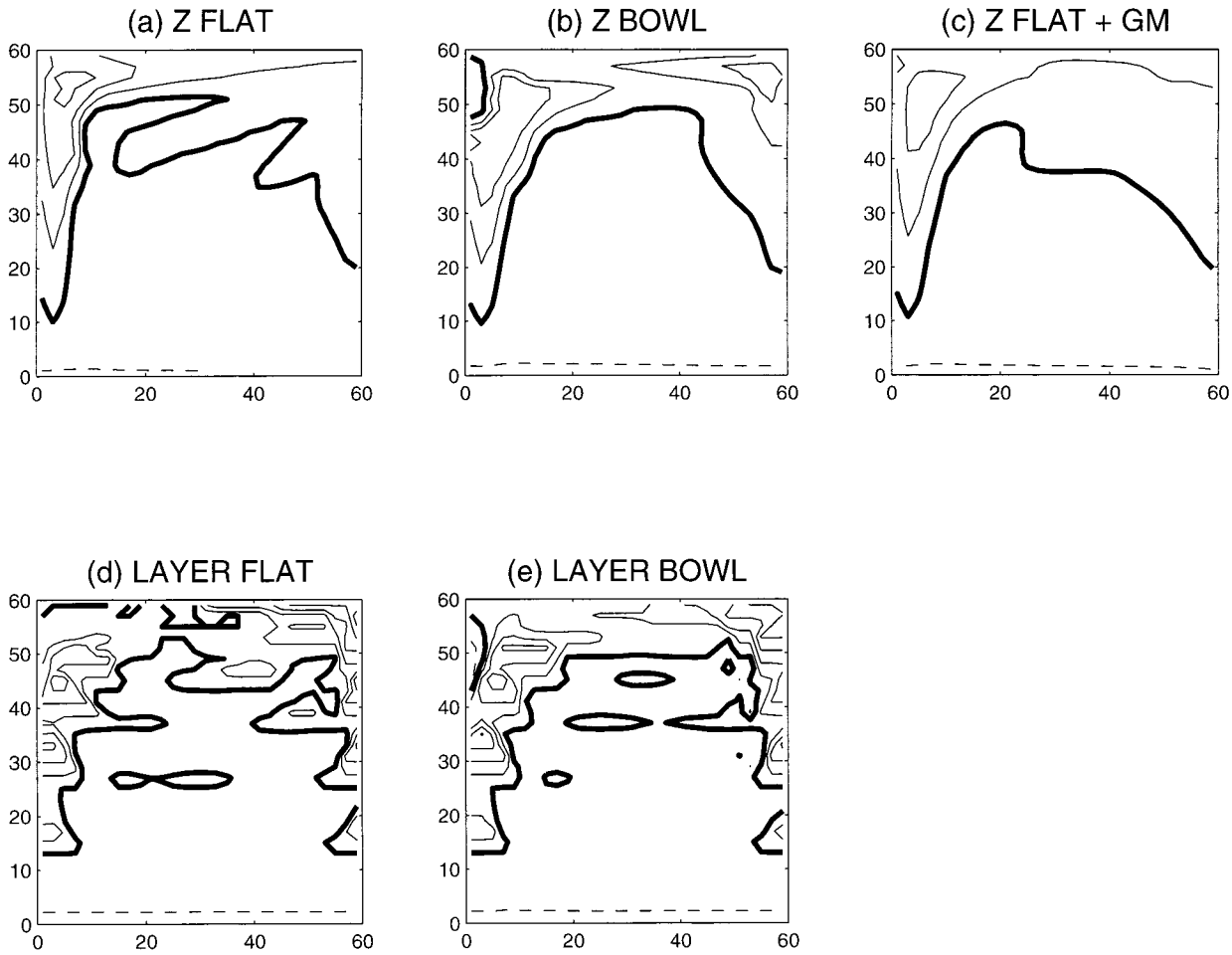

FIG. 6. Surface heat flux pattern when $\kappa = 1 \times 10^{-4}$ m^2 s^{-1} from (a) the z model with flat bottom, (b) the z model with the bowl-shaped basin, (c) the z model with flat-bottom and GM parameterization, (d) the layered model with flat bottom, and (e) the layered model with the bowl-shaped basin. Contour intervals are 40 W m^{-2}. Thick lines are for zeros, dashed lines are for positive values, and the solid lines are for negative values, which means the ocean is losing heat to the air.

supports weak poleward flow. Our conclusion is that the GM parameterization has the expected effect in reducing the differences caused by the differences in the convective mixing parameterization. The effect is quantitatively weak for a realistic range of the horizontal mixing coefficient because, when the convective mixing is strong, a ''slope limiter,'' which disables the GM parameterization when the isopycnal slope is large, becomes effective.

b. Surface heat flux

An overall view of the surface heat flux is shown in Fig. 6, which can be compared directly with the surface circulation shown in Fig. 2. The heat flux patterns from the layered model are quite irregular relative to those from the z model. This is an artifact of the outcrops and it is consistent with irregularities in the surface velocity patterns shown in Fig. 2 and the meridional heat transport profiles shown in Part I. All five cases have certain features in common. For example, heat loss shown by solid lines is mainly confined to the poleward portion of the basin and has much more structure than the almost uniform heat gain in lower latitudes. All five cases show a maximum heat loss associated with the poleward western boundary current. Striking differences in the patterns show up at the eastern boundary at higher latitudes. The standard case for the z model shown in Fig. 6a shows very little heat loss along the eastern boundary. This is also true for the standard case modified by the GM parameterization shown in Fig. 6c. All the other cases show strong heat loss along the eastern boundary, associated with the vigorous eastern boundary currents.

This eastern boundary current also modifies the location of the coldest surface water or deep water mass formation region. In the standard case for the z model, as the western boundary current continues to the east along the northern wall, the water temperature gradually becomes colder and closer to that of the air. The air–sea heat exchange becomes smaller and the coldest wa-

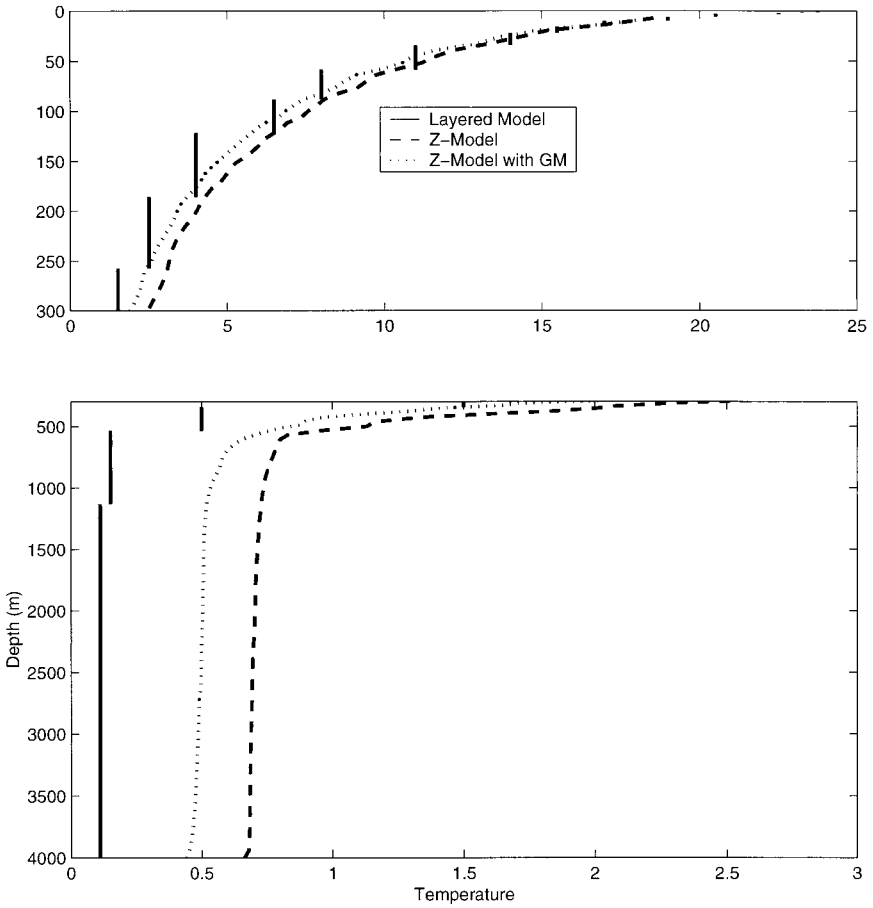

FIG. 7. Rearranged temperature profiles when $\kappa = 0.1 \times 10^{-4}$ m^2 s^{-1}. This is the minimum potential energy state.

ter is observed in the northeast corner of the basin. In the standard case of the layered model, the warm northward eastern boundary current that turns cyclonically along the poleward boundary pushes the location of the coldest water to the west. This effect of the cyclonic flow on the location of the coldest water is strongest in the bowl-shaped bottom cases where the isobaths can guide this boundary flow, as evident from Fig. 2. The area of the coldest water is pushed farther to the western wall and small patches of positive heat flux are observed near the northwestern corner, as indicated in Figs. 6b and 6e.

An important property of the models discussed in Part I of this study is that zonal averages of the heat loss from the surface remain nearly the same in all cases in spite of the different patterns of surface heat flux shown in Fig. 6. Thus the heat loss at the western boundary in Fig. 6a is more intense and extends to higher latitudes, compensating the absence of subpolar heat loss at the eastern boundary found in the other cases.

c. Water mass properties

The different treatment of convection in the two models gives rise to very different deep water properties. Figure 7 is a volumetric census of density in the flat bottom cases. The height range for each density category is proportional to the total volume occupied by that density. In general, the deep water in the layered model is cooler. The lower panel of Fig. 7 shows that the coldest deep water is formed in the standard case of the layered model, and that for the *z* model is about 0.5°C warmer. The deep-water mass properties of a model are very important when making a comparison with observations since they occupy such a large fraction of the oceans. The coldest water that the layered model can represent is predetermined by the layer configuration, and the layered model may be able to produce colder water if a different layer configuration is used.

These differences in water temperature mainly reflect differences in boundary currents due to convection as explained earlier. In the layered model, the eastern boundary current is the main warm water supply to the northern region, while in the *z* model the western boundary current is the main supply, as sketched in Fig. 1. The eastern boundary current, which is fed by the eastward interior flow, is cooler than the western boundary current because the interior zonal flow, which stems

from the western boundary current, equilibrates with the air temperature and becomes cooler while crossing the basin. In the layered model, the supply of warm water to the northern region is smaller. The deep water is formed with less entrainment of warm water and the deep water of the layered model is colder than that of the *z* model. In the *z* model, the GM parameterization weakens the warm western boundary current while enhancing the cold eastern boundary current. The deep-water temperature of the *z* model with the GM parameterization is intermediate between the layered model and the *z* model.

d. Vertical structure

Profiles of zonal velocity u, meridional velocity v, and temperature T for the western and eastern boundaries and the interior are shown in Fig. 8. Figure 8b for the interior shows two zero crossings, separating an intermediate flow to the southwest from abyssal flow below and surface flow to the northeast. The upper zero crossing line for v fluctuates while that for u does not, so a well-defined level of no motion near the surface cannot be obtained. The deeper zero crossings from u and v, however, do coincide well, yielding a well-defined level of no motion, which deepens to the north. In midlatitudes this deepening is quite similar to that of an isotherm. As described in Colin de Verdière (1988, Fig. 6c), the model results show that away from the western boundary and the outcropping area, the potential vorticity is rather uniform on an isothermal surface. As is well known, the potential vorticity constraint makes layers thicken to the north and isothermal surfaces deepen to the north.

The velocity has the structure predicted by the Stommel and Arons (1960) model within the main thermocline and the abyss. The abyssal waters flow eastward and poleward as would be expected in response to upwelling in the main thermocline. The intermediate waters flow southwestward in the opposite direction. A new feature is eastward flow at the surface due to the imposition of the surface boundary condition. The profiles show the familiar beta-spiral structure (Schott and Stommel 1978) in response to upward motion in the interior. At the eastern boundary the flow is similar to that in the interior with two zero crossings, but is compressed toward the surface. The striking difference between the v components at the surface near the eastern boundary as shown in Fig. 3 is evident in the middle panel of Fig. 8c. Another difference is the westward flow at the subsurface or in the main thermocline as shown in the middle panel of Fig. 8b. In the *z* model the westward flowing intermediate waters not only compensate abyssal flow, but this westward flow also compensates eastward flowing surface water, which downwells in the unstratified or weakly stratified region at the eastern boundary. Therefore the standard *z* model shows a stronger intermediate westward flow then the layered model. The *z* model with the GM parameterization suppresses this sinking near the eastern boundary and the subsurface westward flow becomes weaker. The flow at the western boundary is less complex. It is mainly poleward flow at the surface compensated by equatorward flow at depth as predicted by the two-layer model of Stommel and Arons (1962).

e. Diapycnal velocity

Zonal sections of diapycnal velocity, w^*, and temperature at 30°N from flat bottom cases are shown in Fig. 9. At the surface near the western boundary of the layered model the ocean loses heat to the air so that the water becomes cold. This is associated with negative values of w^* near the surface in this area. Similar heat loss also takes place near the eastern boundary, with corresponding negative values of w^* near the surface. When the zonal flow from the west meets the eastern boundary, the isotherms are pushed downward, causing the temperature profile to be concave downward. This also contributes to negative w^*. The downwelled water returns to the west as intermediate water, which effects the temperature profile farther offshore, forming a tongue of negative w^* in the subsurface, as shown in Fig. 9a.

Excluding these two patches of negative w^* near the meridional walls at high latitudes, w^* is almost uniformly positive over most of the thermocline, consistent with the Stommel and Arons model. Near the eastern boundary at the base of the convectively mixed layer, convection and upwelling cause the vertical gradient in temperature to become a maximum. High potential vorticity water forms near the base of the mixed layer and spreads to the southwest as a tongue, as described in the planetary geostrophic model of Colin de Verdière (1988).

The diapycnal velocity, w^*, is much more difficult to analyze in the *z* model. The vertical velocity must be projected onto isopycnal surfaces. Near the western boundary the slope of isopycnal surfaces are too large to obtain an accurate estimate, and the western boundary is omitted in Fig. 9c. In the *z* model, we suppressed horizontal diffusivity by adopting the flux-corrected transport. Therefore, numerical diapycnal diffusion due to the Veronis effect (Veronis 1975) is not significant in the western boundary. In general, the distribution of w^* in the interior is similar to that of the layered model, but the magnitude is less. There appears to be a larger area of negative w^* near the eastern boundary, even though there is very little heat loss at the surface, because the convective adjustment removes the vertical stratification and makes vertical motion easier. As it is shown in Part I, the total diapycnal flux along latitude circles on an isotherm is the same in the two models, and the low interior values of the *z* model must be compensated by higher values near the western boundary. Although κ, the vertical diffusivity, is constant

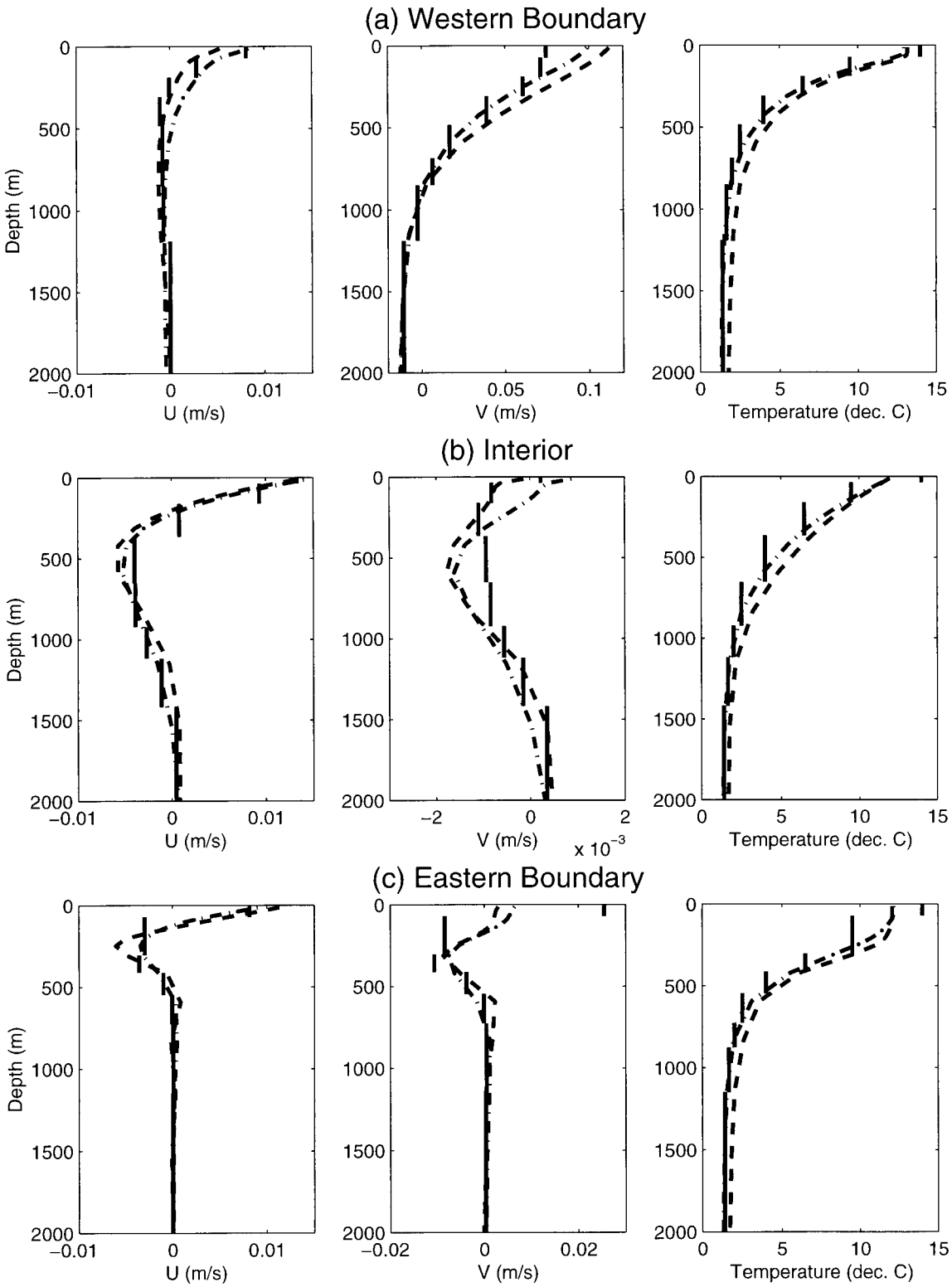

FIG. 8. Vertical profiles of velocity and temperature from runs with the flat-bottom geometry when $\kappa = 1 \times 10^{-4}$ m^2 s^{-1}: (a) within the western boundary, (b) average over from 20° to 40°E and from 20° to 40°N, and (c) in the eastern boundary. Solid lines are for the layered model, dashed curves are for the standard z model, and dash-dotted curves are for the z model with the GM parameterization.

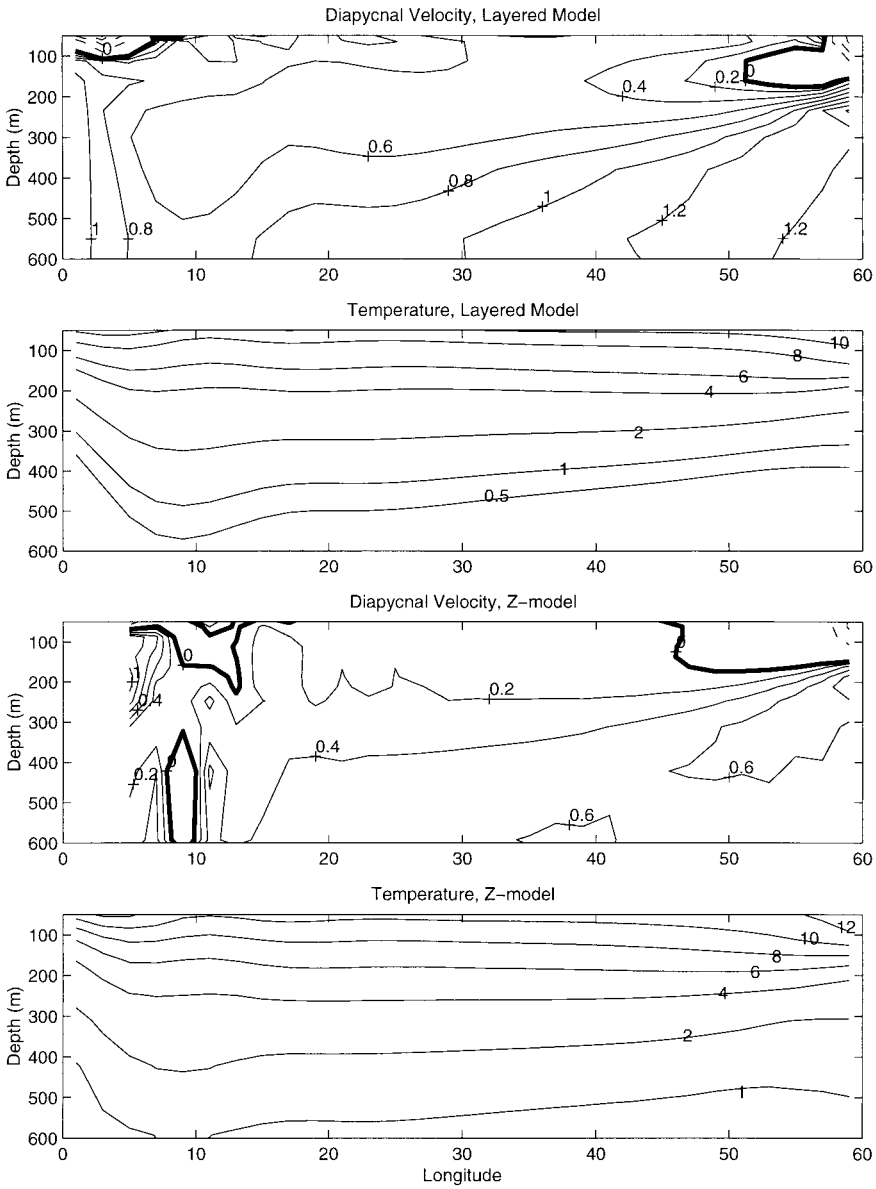

FIG. 9. Zonal sections of diapycnal velocity at 30°N from (a) the layered model and (c) the z model, and temperature from (b) the layered model and (d) the z model with flat-bottom geometry when $\kappa = 0.1 \times 10^{-4}$ m^2 s^{-1}. In (a) and (c), solid contours represent positive values and dashed contours are for negative values. The contour interval for the dashed curves, which represent negative values, is 2, while for the solid curves, which are for positive values, it is -0.2, in the unit of 10^{-7} m^2 s^{-1}.

throughout the domain, diapycnal flux is concentrated along the western boundary. This also suggests that in the z model controlling the spatial distribution of vertical mixing may not be obtained by a simple modification of spatial distribution of κ.

3. Summary and conclusions

A comparison of different numerical models of the North Atlantic (DYNAMO Group 1997) shows that codes with quite different vertical coordinate systems indicated quite similar results at lower latitudes where the ocean is well stratified. In high latitudes, however, where convection and intermediate and deep water formation take place, the codes give quite different results. Using a very simplified physical model, which can be considered an extension of the Stommel and Arons/Kawase abyssal flow model, this study makes a similar comparison of ocean circulation codes using both level coordinates and coordinates based on isopycnal surfaces. The classical abyssal flow model is extended to three dimensions by including a specified buoyancy forcing

at the surface using the Newtonian damping condition. If wind forcing is not included, it is shown in Part I of this study that numerical experiments for this thermohaline circulation model obey simple scaling laws proposed by Bryan and Cox (1967) and Welander (1971). Zonally integrated quantities are in surprisingly good agreement for the two codes based on level and isopycnal coordinates.

In Part II we have concentrated on the three-dimensional aspects of the circulation predicted by the two codes. The findings for our very simple thermocline model are in accord with the DYNAMO Group (1997). In lower latitudes the two codes give very similar results, and the pattern of flow in the intermediate and deep water is in basic accord with the Stommel and Arons/Kawase model. At the surface in higher latitudes where convection is dominant the circulation patterns are very different. For the *z* model, deep sinking takes place at the poleward boundary near the eastern wall, and almost no surface cyclonic circulation is indicated. The pattern is similar to that shown in previous studies of Cox and Bryan (1984) and Colin de Verdière (1988). On the other hand, the isopycnal code shows a small cyclonic gyre in subpolar latitudes and the sinking takes place along the poleward wall near the western boundary.

That convection is important only in the subpolar region of the models and that differences exist mostly in the subpolar regions is circumstantial evidence that different convective parameterizations in the two models are responsible. The *z* model uses convective adjustment, which mixes in the vertical, leading to a homogeneous water column, whenever vertical static instability is indicated. On the other hand, the convection in the layered model causes a thinning of the upper layer and a thickening of the adjacent layer below. The result is to cool the water column while maintaining some stratification. These two parameterizations of convection are quite different, and merely increasing the vertical resolution does not lead to convergence.

The results of this study have many implications for interpreting ocean circulation models and the simulation of climate at higher latitudes with coupled models. In a very simple model it has been shown that models with different convective parameterizations produce very different circulation patterns in subpolar latitudes in response to the same surface buoyancy. The convective parameterizations are shown to be as important as the architecture of the model. Convection in the layer model leads to subpolar surface cyclonic circulation with deep sinking in the northwest corner of a Northern Hemisphere basin. Convective adjustment, which is the most commonly used parameterization, inhibits the formation of a subpolar cyclonic gyre and leads to deep sinking in the northeast corner of the basin. The Gent and McWilliams (1990) parameterization of mesoscale eddies modifies the effect of the convective adjustment, restoring the stratification to some extent and allowing a weak surface cyclonic cell to form.

In the *z* model, as in Winton (1997) and Spall and Pickart (2001), we need to introduce shelves along the boundaries to get a polar cyclonic gyre, and move the water mass formation region to the northwest corner. The shelf along the eastern boundary, however, cannot make the eastern boundary stratified. In the layered model the circulation in the polar ocean is cyclonic and water mass formation occurs near the northwest corner, even in the flat bottom case. Of course, the experiments presented in this paper are different from reality, and the boundary conditions in our simplified models are only a very crude analog of the actual boundary conditions of the Atlantic. In the subpolar area, however, where buoyancy forcing becomes dominant (Luyten et al. 1985), it is significant that it was impossible to simulate any cyclonic surface circulation in the *z* model, while the layered model does have a circulation near the surface at the poleward boundary, much more like what is observed in the real ocean. A laboratory experiment by Park and Whitehead (1999) on thermally driven circulation also shows flow equivalent to northward eastern boundary current. We show that the difference in the two models is due to the convection parameterization.

Diapycnal velocity across isotherms proved to be quite difficult to analyze in the *z* model, but the results suggested that the diapycnal velocity is much less consistent with ideal models of the abyssal circulation. Much of the diapycnal flux appears to take place near the western boundary, although κ is uniform throughout the basin. This suggests that in the *z* model we may not be able to control the spatial distribution of vertical mixing by changing the the distribution of κ. In the layered model, the distribution of w^* is more uniform and consistent with the ideal abyssal circulation models. It appears that an isopycnal model is a much better tool for future studies of vertical mixing and diapycnal flow.

The results of this study show that models of ocean circulation are quite sensitive to the architecture of the the numerical model. It suggests that future studies should be carried out using more than one numerical approach to insure that the conclusions drawn from the calculations are robust and not due to special features of the solutions dependent on the vertical structure of the model or the way in which convection or the mixed layer is handled. In other words, one should not trust just one model, but carry out studies using several model architectures and several different types of convection schemes. We expect that coupled ocean–atmosphere models of climate will be even more sensitive to details of model architecture than models in which the upper boundary of the ocean is highly constrained by climatological data. At present carrying out a modeling study with more than one model is technically quite difficult. The DYNAMO Project (DYNAMO Group 1997) and this study show that future model development should

aim to build more general ocean modeling tools that will allow several model architectures within one model framework.

Acknowledgments. We wish to thank to R. Hallberg, S. Griffies, R. Pacanowski, and A. Gnanadesikan for their help with the models, useful discussions, and suggestions. We also thank P. Goodman and an anonymous reviewer for their comments and suggestions. Calculations were performed using the GFDL/NOAA computing facilities while Y.-G. Park was supported by GFDL–Princeton University Visiting Scientist Program. Y.-G. Park also received partial support from the Climate Environment Research Center sponsored by the SRC program of Korea Science and Engineering Foundation. K. Bryan was supported by DOE Grant ER61920-1004726-000026. A part of this paper was prepared while Y.-G. Park was at the Center for Ocean–Land–Atmosphere Studies.

REFERENCES

Bleck, R., and L. T. Smith, 1990: A wind-driven isopycnic coordinate model of the North and equatorial Atlantic Ocean; 1. Model development and supporting experiments. *J. Geophys. Res.,* **95,** 3273–3285.

Bryan, K., 1989: The design of numerical models of the ocean circulation. *Oceanic Circulation Models: Combining Data and Dynamics*, D. L. T. Anderson and J. Willebrand, Eds., Kluwer Academic, 465–500.

——, and M. D. Cox, 1967: A numerical investigation of the oceanic general circulation. *Tellus*, **19,** 54–80.

Colin de Verdière, A., 1988: Buoyancy driven planetary flows. *J. Mar. Res.*, **46,** 215–265.

Cox, M. D., and K. Bryan, 1984: A numerical model of the ventilated thermocline. *J. Phys. Oceanogr.,* **14,** 674–687.

DYNAMO Group, 1997: DYNAMO: Dynamics of North Atlantic Models: Simulation and assimilation with high resolution models. Tech. Rep. No. 294, Institut für Meereskunde, Kiel, Germany, 334 pp.

Gent, P. R., and J. C. McWilliams, 1990: Isopycnal mixing in ocean circulation models. *J. Phys. Oceanogr.,* **20,** 150–155.

Hallberg, R., 2000: Time integration of diapycnal diffusion and Richardson number–dependent mixing in isopycnal coordinate ocean models. *Mon. Wea. Rev.,* **128,** 1402–1419.

——, and R. Peter, 1996: Buoyancy-driven circulation in an ocean basin with isopycnals intersecting the sloping boundary. *J. Phys. Oceanogr.,* **26,** 913–940.

Haney, R. L., 1974: A numerical study of the response of an idealized ocean to large-scale surface heat and momentum flux. *J. Phys. Oceanogr.,* **4,** 145–167.

Kawase, M., 1987: Establishment of deep ocean circulation driven by deep water. *J. Phys. Oceanogr.,* **17,** 2294–2317.

Luyten, J., H. M. Stommel, and C. Wunsch, 1985: A diagnostic study of the northern Atlantic subpolar gyre. *J. Phys. Oceanogr.,* **15,** 1344–1348.

Pacanowski, R. C. P., 1995: MOM2 documentation. User's guide and reference manual. GFDL Ocean Tech. Rep. No. 3, Princeton, NJ, 232 pp.

Park, Y.-G., and J. A. Whitehead, 1999: Rotating convection driven by differential bottom heating. *J. Phys. Oceanogr.,* **29,** 1208–1220.

——, and K. Bryan, 2000: Comparison of thermally driven circulations from a depth-coordinate model and an isopcnal-layer model. Part I: Scaling-law sensitivity to vertical diffusivity. *J. Phys. Oceanogr.,* **30,** 590–605.

Salmon, R., 1990: The thermocline as an ''internal boundary layer.'' *J. Mar. Res.,* **48,** 437–469.

Samelson, R. M., and G. K. Vallis, 1997: Large-scale circulation with small diapycnal diffusion: The two-thermocline limit. *J. Mar. Res.,* **55,** 223–275.

Schott, F., and H. Stommel, 1978: Beta sprial and absolute velocities in different oceans. *Deep-Sea Res.,* **25,** 961–1010.

Spall, M. A., and R. S. Pickart, 2001: Where does dense water sink? A subpolar gyre example. *J. Phys. Oceanogr.,* **31,** 810–826.

Stommel, H., and A. B. Arons, 1960: On the abyssal circulation of the world ocean. II—An idealized model of the circulation pattern and amplitude in oceanic basins. *Deep-Sea Res.,* **6,** 217–233.

——, and J. Webster, 1962: Some properties of thermohaline equations in a subtropical gyre. *J. Mar. Res.,* **20,** 42–56.

Veronis, G., 1975: The role of models in tracer studies. *Numerical Models of Ocean Circulation,* Natl. Acad. of Sci., 133–146.

Welander, P., 1971: The thermocline problem. *Philos. Trans. Roy. Soc. London,* **A270,** 415–421.

Winton, M., 1996: The role of horizontal boundaries in parameter sensitivity and decadal-scale variability of coarse-resolution ocean general circulation models. *J. Phys. Oceanogr.,* **26,** 289–304.

——, 1997: The damping effect of bottom topography on internal decadal-scale oscillations of the thermohaline circulation. *J. Phys. Oceanogr.,* **27,** 203–208.